

---

# Compact Attention: Exploiting Structured Spatio-Temporal Sparsity for Fast Video Generation

---

**Qirui Li<sup>1†</sup>, Guangcong Zheng<sup>1†</sup>, Qi Zhao<sup>1</sup>, Jie Li<sup>1</sup>, Bin Dong<sup>2</sup>, Yiwu Yao<sup>2</sup>, Xi Li<sup>1</sup>**

<sup>1</sup>College of Computer Science & Technology, Zhejiang University

<sup>2</sup>Huawei Technologies

{qirui.l, guangcongzheng}@zju.edu.cn

## Abstract

The computational demands of self-attention mechanisms pose a critical challenge for transformer-based video generation, particularly in synthesizing ultra-long sequences. Current approaches, such as factorized attention and fixed sparse patterns, fail to fully exploit the inherent spatio-temporal redundancies in video data. Through systematic analysis of video diffusion transformers (DiT), we uncover a key insight: Attention matrices exhibit structured, yet heterogeneous sparsity patterns, where specialized heads dynamically attend to distinct spatiotemporal regions (e.g., local pattern, cross-shaped pattern, or global pattern). Existing sparse attention methods either impose rigid constraints or introduce significant overhead, limiting their effectiveness. To address this, we propose **Compact Attention**, a hardware-aware acceleration framework featuring three innovations: 1) Adaptive tiling strategies that approximate diverse spatial interaction patterns via dynamic tile grouping, 2) Temporally varying windows that adjust sparsity levels based on frame proximity, and 3) An automated configuration search algorithm that optimizes sparse patterns while preserving critical attention pathways. Our method achieves  $1.6 \sim 2.5\times$  acceleration in attention computation on single-GPU setups while maintaining comparable visual quality with full-attention baselines. This work provides a principled approach to unlocking efficient long-form video generation through structured sparsity exploitation. **Project Page:** <https://yo-ava.github.io/Compact-Attention.github.io/>

## 1 Introduction

The rapid advancement of generative models has enabled high-quality video synthesis; however, processing ultra-long sequences remains a critical bottleneck. For Transformer-based video generation models, the quadratic complexity of self-attention mechanisms presents a fundamental challenge, as modeling spatiotemporal dependencies requires handling extensive token sequences. For example, in the Hunyuan-video architecture [19], generating a 128-frame 720p HD video entails processing over 100K tokens, with attention computation consuming 68-72% of the total generation time. This computational burden becomes prohibitive for long-form video generation, necessitating the development of innovative acceleration strategies.

Recent studies [61, 47, 13, 46, 8, 60, 54] show that full attention matrices in video generation exhibit significant sparsity, with complex distributions of attention weights and structured yet seemingly irregular patterns (Fig. 1), indicating substantial untapped acceleration potential. The primary challenge lies in effectively leveraging these heterogeneous sparse patterns. Even if accurate predictions can be made, the overhead associated with locating the sparse locations often offsets the potential speed gains.

---

<sup>†</sup>These authors contributed equally to this work.

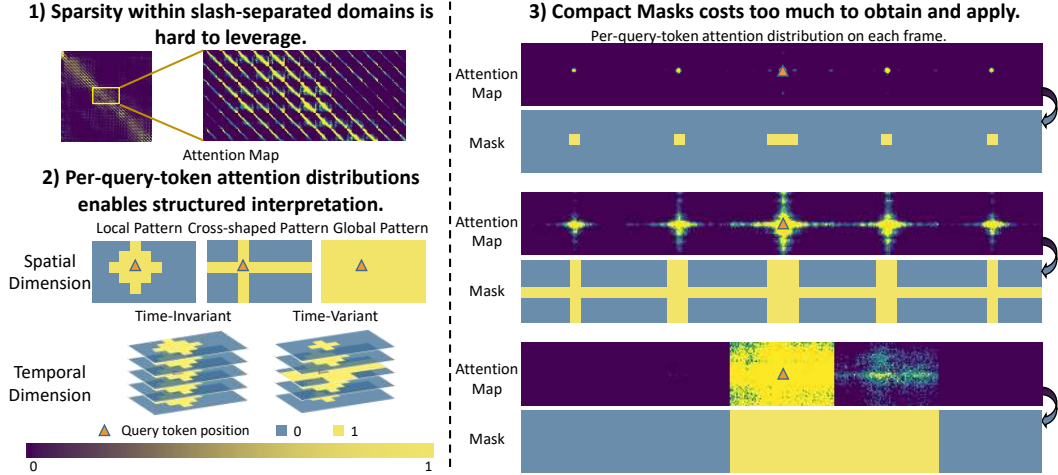


Figure 1: Sparsity between slashes are hard to exploit for acceleration. Periodic, hierarchical attention patterns are shown in complicated attention maps when a single query token is arranged properly.

Our analysis of video diffusion transformers (DiT) uncovers a critical phenomenon: the interaction between 3D spatiotemporal token sequences may induce periodic, hierarchical attention patterns. As shown in Fig. 1, specialized attention heads emerge with distinct functional roles: focusing on local spatial regions, forming cross-shaped spatial interactions, and exhibiting a global or input-related focus. Additionally, certain heads exhibit relationships with frames at specific relevant distances. Some attention heads demonstrate temporal locality by suppressing distant frames, while others do the opposite. These structured sparsity patterns present opportunities for efficient approximation, however, existing methods fail to fully exploit these patterns.

Previous approaches, such as Minference[15], generalize sparse attention from language models by using fixed patterns (e.g., diagonals, blocks), but when applied to video generation, they overlook the unique 3D redundancies inherent in video data. Spurge Attention[60] improves spatial grouping through Hilbert-order flattening and leverages locality, but it introduces additional overhead. SVG [46] recognizes the unique periodic patterns in video data but does not account for the dynamic sparsity exhibited by each attention head. The sliding window approach in STA[61] captures local spatiotemporal correlations but limits attention to rigid cubic regions, thereby missing crucial cross-frame interactions, sparsity related to relative temporal distance, and corresponding redundancies.

These limitations highlight the need for a video-specific sparse attention mechanism that can adaptively capture structured and dynamic spatiotemporal patterns. We summarize our key contributions as follows:

- We reveal structured and hierarchical attention patterns in video diffusion transformers, uncovering specialized spatiotemporal attention behaviors that motivate efficient sparse approximations.
- We propose **Compact Attention**, a training-free sparse attention framework that integrates an offline configuration search strategy with an efficient attention computation mechanism, while preserving the fidelity of generated videos.
- We validate our approach on the Wan2.1 and Hunyuan model, achieving up to **2.5 $\times$**  end-to-end speedup with negligible degradation in generated video quality.

## 2 Related Works

**Acceleration of diffusion models.** Due to the high inference cost, accelerating diffusion models has become a central research focus. Existing methods largely aim to reduce sampling steps and fall into two main categories: improved sampling algorithms [39, 28, 25, 2, 26, 62] and distillation-based approaches [32, 36, 55, 21, 51, 14, 56, 37, 17, 40]. Distillation methods compress multi-step diffusion into a compact student model via teacher-student training, reducing inference steps. Beyond step reduction, several works [30, 1, 45, 23, 31, 29, 16] explore cache mechanisms to eliminate redundant

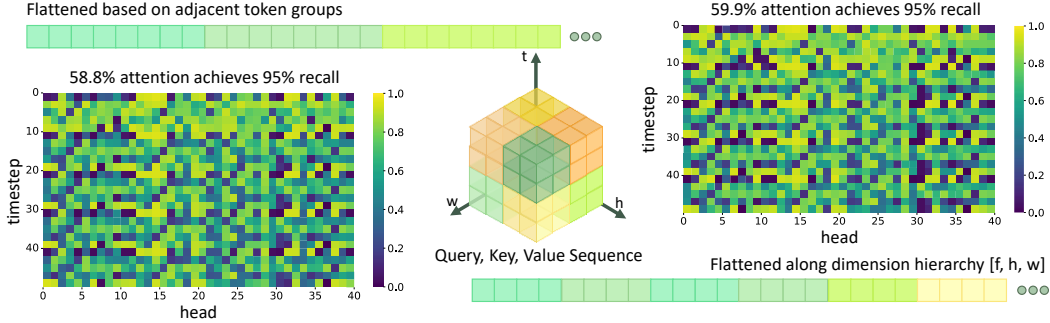


Figure 2: Heatmap of attention map and the  $k\%$  values required to retain top- $k$  for 0.95 recall before and after rearranging attention maps into 3D spatially adjacent groups.

computation. Notably, [31] proposes a learning-based caching (L2C) strategy, while [45] applies block-level caching to reuse layer outputs across steps. DeepCache [30] further leverages temporal redundancy by reusing high-level features and updating only low-level ones. In addition to these approaches, attention-level optimization such as attention quantization and sparsification [64, 22, 58, 59]—offers complementary acceleration potential.

**Sparse attention.** Sparse attention reduces the quadratic complexity of self-attention by masking computations to predefined sparse regions. In large language models, numerous studies [3, 57, 65, 52, 53, 50, 10, 4] have explored sparse attention designs. Some methods [49, 63, 48, 6, 33, 12, 9, 24, 41, 5] use fixed patterns targeting specific positions. For instance, LM Infinite [12], MoA [9], and MAPSparse [24] adopt A-shaped patterns and Ltri-LLM [41] identifies triangular structures. Recognizing the dynamic nature of attention, several works [34, 18, 44, 35, 42, 38, 20, 15, 11] introduce input-adaptive sparse attention. MInference [15], for example, identifies three pattern types—A-shape, Vertical-Slash, and Block-Sparse. In video generation, however, the inherent 3D redundancy poses challenges for directly transferring LLM-based sparse attention methods. Recent efforts [61, 47, 13, 46, 8, 60, 54] target video-specific sparsity. STA [61] adopts a sliding window for local spatiotemporal attention but underutilizes the full 3D redundancy present in video data.

### 3 Stable Spatiotemporal Patterns Enable Offline Attention Mask Precomputation

#### 3.1 Tile-Based Sparsity for Efficient Blockwise Attention

Although attention exhibits significant sparsity, performing sparse predictions in a token-by-token manner is impractical for real-world acceleration scenarios due to the substantial overhead introduced by both prediction and execution processes. We observe that critical information within attention maps tends to cluster in three-dimensional space. Considering low-level computational efficiency, processing data in a block-wise manner simultaneously exploits the clustering characteristics of sparsity, meets acceleration demands, and reduces memory consumption.

We conducted sparsity validation experiments on attention maps, analyzing various timesteps and layers within T2V models Wan1.2 [43] and Hunyuan [19]. More results are shown in appendix D. By comparing two flattening strategies—directly flattening the three-dimensional sequence  $(f, h, w)$  into a one-dimensional sequence versus grouping and flattening based on spatially adjacent tiles in 3D space[61] (as illustrated in Fig. 2)—We observe that the latter reduces the average number of blocks required to retain the top- $k$  values for 0.95 recall by **1.1%** in the Wan2.1 model, increasing to **3.4%** in the Hunyuan model, while preserving a high overall sparsity rate and maintaining compatibility with block-wise attention mechanisms.

#### 3.2 Structured Spatiotemporal Patterns in Attention Maps

The attention maps derived from 1D sequences with 3D structural information  $(f, h, w)$  exhibit highly complex morphological diversity. Existing sparse attention methods in video generation models have identified clustering patterns such as slash-line, vertical-line, and block-shaped formations in these

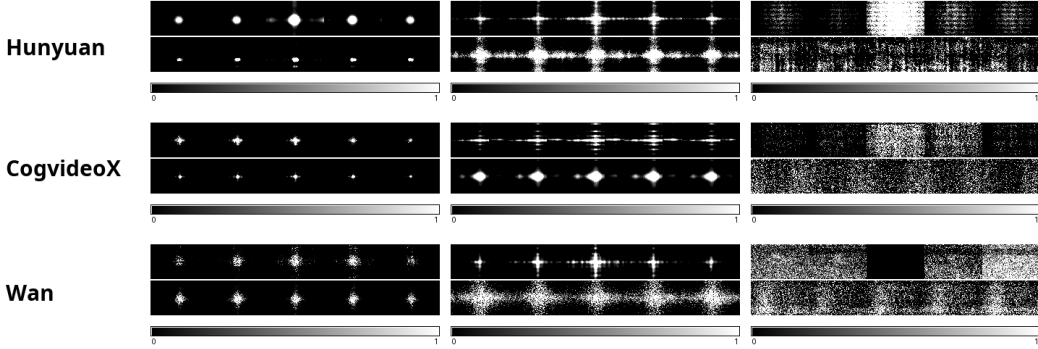


Figure 3: Three characteristic attention patterns observed in video transformers: local pattern (left), cross-shaped pattern(middle) and global pattern(right) with the upper one showing temporal dynamics while lower one being persistent along frames. Each Attention map is shown using query of the token in the middle and keys from the other tokens.

attention maps, and have subsequently designed minimal pattern primitives (e.g., vertical stripes, slash stripes, and blocks) to approximate these sparse motifs. However, a fine-grained analysis of per-query-token attention distributions facilitates a structured interpretation of the intricate patterns within the attention maps. By examining full attention maps at the query-specific token level, we observe that diagonal patterns arise from systematic position-relative attention biases, which visually manifest as distinct spatiotemporal modes. Through empirical analysis, we identify three dominant spatial patterns and two temporal patterns that are commonly present in 3D full-attention video generation models (as illustrated in Fig. 3).

#### Spatial Patterns:

- **Local Patterns:** Certain attention heads focus on compact neighborhoods around target positions, forming spherical attention fields that are likely crucial for fine-grained detail synthesis.
- **Cross-Shaped Patterns:** Specialized attention heads exhibit directional sensitivity, creating continuous attention corridors along the horizontal and vertical axes.
- **Global Patterns:** Some attention heads preserve full spatial connectivity irrespective of the relevant distance. Additionally, input-dependent attention heads exhibit strong weight clustering around salient objects, which are also observed as global patterns.

#### Temporal Patterns:

- **Time-Variant Patterns:** This pattern exhibits a strong correlation with temporal relative distance. Some attention heads demonstrate progressive weight decay across frames, while others focus more on frames at a specific distance, excluding local or nearby frames.
- **Time-Invariant Patterns:** These attention heads maintain frame-agnostic distributions, ensuring a consistent focus across all timesteps regardless of the relative temporal distance.

### 3.3 Pattern Stability Enables Offline Acceleration

Our systematic analysis demonstrates that spatiotemporal attention patterns arise as inherent properties of the model architecture, rather than being driven by input adaptations.

The attention patterns demonstrate significant stability across various layers and heads within a video generation model. We define pattern classification using a recall-based threshold criterion: attention mechanisms that cover more than 85% of the spatial extent are classified as global patterns, while smaller, more concentrated regions correspond to local interaction modes.

- **Local Patterns:** focus around query positions  $(x_t, y_t)$  with axes-aligned constraints.  $\omega$  and  $\eta$  denote boundaries of patterns:

$$\mathcal{R}_{\text{local}} = \left\{ (x, y) \mid \max \left( \frac{|x - x_t|}{\omega}, \frac{|y - y_t|}{\eta} \right) \leq 1 \right\} \quad (1)$$

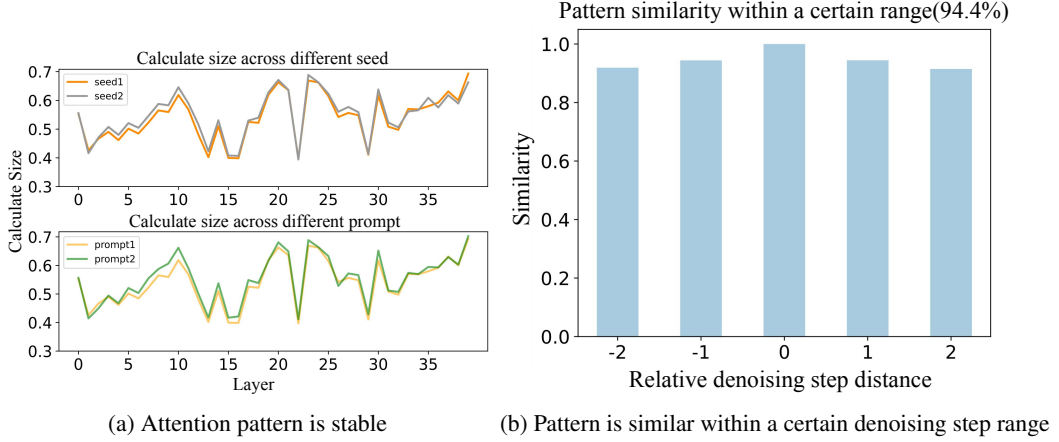


Figure 4: (a) A visualization of the layer-wise computation during denoising. For different prompts, the computational demands are nearly identical. (b) Region similarity across denoising steps.

- **Cross-shaped Pattern:** Cross-shaped regions with complementary spatial constraints:

$$\mathcal{R}_{\text{cross}} = \left\{ (x, y) \mid \bigvee_{k=1}^2 \left( \frac{|x - x_t|}{\omega_k} \leq 1 \wedge \frac{|y - y_t|}{\eta_k} \leq 1 \right) \right\} \quad (2)$$

where  $(\omega_1 - \omega_2)(\eta_1 - \eta_2) < 0$  enforces complementary axis dominance.  $\omega_k$  and  $\eta_k$  denote boundaries of patterns.

**Input/Seed Invariance.** As demonstrated in Fig. 4a, sizes of pattern regions stay alike with average similarity over 0.8 across varying text prompts and random initializations, measured by:

$$\text{Sim}(M_A, M_B) = \frac{\|M_A \odot M_B\|_1}{\|M_A + M_B - M_A \odot M_B\|_1} \quad (3)$$

where  $M_A, M_B$  are binarized attention masks.

**Temporal Robustness.** As shown in Fig. 4b, attention configurations remain stable within a certain range across denoising steps, enabling reliable offline pre-computation of attention masks optimized per model-layer-head combination.

## 4 Compact Attention

### 4.1 Tile-based Deformable Sparse Pattern

Building upon the spatio-temporal patterns identified in Section 3, we propose an adaptive tile-based strategy that effectively captures complex attention distributions while preserving hardware efficiency. Our approach fundamentally reconsiders the interaction between sparse attention patterns and the intrinsic structure of video data. Instead of relying on rigid, predefined attention windows, we allow sparse configurations to dynamically adapt across both spatial and temporal dimensions.

The core innovation of our method is conducted based on a hierarchical grouping mechanism that respects the dual nature of video data—temporal variation and spatial locality. By reorganizing tokens into spacetime tiles—clusters of tokens that are adjacent in both spatial and temporal domains—we construct computational units that align with the natural locality inherent in video content. This tile abstraction serves as the foundational building block for constructing deformable attention patterns.

**Frame-Group-wise Patterns:** To capture temporal dynamics, we partition frames into distance-based groups relative to the current frame being processed, with each group governed by its own sparse configuration. **Dual Attention Windows:** Within each group, spatial attention masks are adaptively composed from two complementary window shapes that approximate the observed attention patterns (e.g., cross-shaped, local blocks). This design eliminates the need for explicit pattern classification during inference.

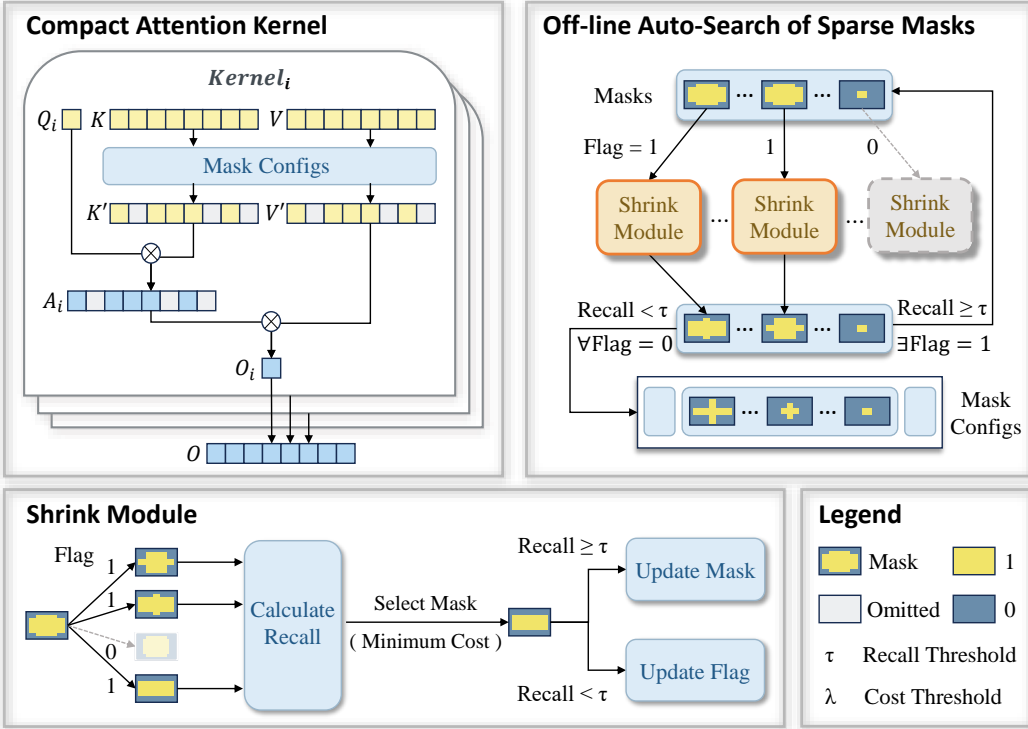


Figure 5: Compact Attention: Pipeline

This deformable architecture achieves a three-fold synergy: (1) spatial adaptability through tile combinations that emulate diverse attention modes, (2) temporal awareness via distance-stratified configurations, and (3) hardware efficiency by preserving the computational regularity inherent in tile-based processing.

## 4.2 Optimized Auto-Search of Sparse Masks

Our mask search framework addresses two fundamental challenges: (1) the prohibitive computational overhead of online mask prediction, and (2) the stability of attention patterns across diverse inputs (as discussed in Section 3). The key insight lies in decoupling pattern discovery from runtime execution through an offline configuration pipeline that preserves spatiotemporal coherence. The whole pipeline is shown in Fig. 5.

Guided by the spatial variation characteristics presented in Section 3, we formulate mask optimization as a boundary contraction process along hierarchical dimensions. The process starts with full attention coverage and iteratively tightens window boundaries across spatial dimensions, prioritizing regions with lower recall contributions, as indicated by the recall loss per computational unit (cost). This directional shrinkage operates independently across different frame groups.

The contraction process is governed by dual thresholds: a minimum recall threshold  $\tau$ , which preserves critical interactions, and a maximum cost threshold  $\lambda$ , which balances computational reduction against accuracy loss. The mask shrinking process for a given frame group terminates when either the recall drops below  $\tau$  or the cost of further shrinking ( $\Delta Recal / \Delta Cost$ ) exceeds  $\lambda$ , ensuring an effective trade-off between quality and efficiency. To obtain the final configuration, we merge configurations across prompts through union operations (see Section 6). This conservative merging strategy guarantees that all potentially relevant attention regions are retained.

Capitalizing on the temporal stability of diffusion trajectories (see Fig. 4b), we implement mask reuse across  $n$  consecutive denoising steps. This configuration caching mechanism reduces the search frequency by  $n \times$ , while maintaining generated video quality.

Table 1: Comparative Analysis of Sparse Attention Methods for Text-to-Video Models. Compact Attention achieves faster high-quality video generation compared with methods with higher sparsity.

Model	Method	Sparsity	Quality			Speed	
			SSIM $\uparrow$	PSNR $\uparrow$	MSE $\downarrow$	Latency (s)	Speedup
Wan2.1 (80K)	Full Attention	0%	-	-	-	1092.168	1.00x
	Sparse VideoGen	32.08%	0.529	15.9564	1894.3672	1200.148	0.91x
	SpurgeAttn	32.27%	0.6102	20.5163	676.0723	1065.796	1.02x
	<b>Compact Attention(Ours)</b>	33.99%	0.7754	23.7297	351.6015	<b>663.824</b>	<b>1.65x</b>
	<b>Compact Attention(Ours)</b>	24.66%	<b>0.8147</b>	<b>25.2664</b>	<b>254.1789</b>	758.176	1.44x
Hunyuan (127K)	Full Attention	0%	-	-	-	1370.658	1.00x
	Sparse VideoGen	50.35%	0.7254	20.4297	822.8567	1117.767	1.23x
	SpurgeAttn	47.77%	0.7794	23.5889	369.3112	1148.628	1.19x
	<b>Compact Attention(Ours)</b>	62.36%	0.9040	30.0822	105.1957	<b>546.504</b>	<b>2.51x</b>
	<b>Compact Attention(Ours)</b>	52.90%	<b>0.9452</b>	<b>34.5506</b>	<b>35.1307</b>	750.201	1.83x

Table 2: Quantitative Comparison of Sparse Attention Methods in Wan2.1 and Hunyuan on VBench: Visual Consistency, Aesthetic Quality and Text-Video Alignment.

Model	Method	Sparsity	Subject	Background	Aesthetic	CLIPSIM	CLIP-T
			Consistency	Consistency	Quality		
Wan2.1 (80K)	Full Attention	0%	0.9681	0.9616	0.6486	0.2118	0.9985
	Sparse VideoGen	32.08%	0.9547	0.9565	0.6380	0.2116	<b>0.9987</b>
	SpurgeAttn	32.27%	0.9357	0.9500	0.5320	0.2064	0.9982
	<b>Compact Attention (Ours)</b>	33.99%	<b>0.9659</b>	<b>0.9650</b>	0.6480	<b>0.2121</b>	0.9985
	<b>Compact Attention (Ours)</b>	24.66%	<b>0.9674</b>	<b>0.9638</b>	<b>0.6459</b>	<b>0.2122</b>	0.9986
Hunyuan (127K)	Full Attention	0%	0.9736	0.9735	0.6542	0.2181	0.9995
	Sparse VideoGen	50.35%	0.9701	0.9722	<b>0.6638</b>	0.2014	0.9995
	SpurgeAttn	47.77%	0.9664	0.9731	0.5794	0.2112	0.9995
	<b>Compact Attention (Ours)</b>	62.36%	<b>0.9716</b>	<b>0.9693</b>	0.6531	<b>0.2184</b>	0.9995
	<b>Compact Attention (Ours)</b>	52.90%	<b>0.9723</b>	<b>0.9735</b>	0.6536	<b>0.2184</b>	0.9995

## 5 Experiments

### 5.1 Experimental Setup

Our evaluations are primarily conducted on the state-of-the-art video generation architecture Wan2.1(14B) and Hunyuan on a single H800 GPU. We apply Compact Attention to generate outputs consisting of 81 frames in Wan2.1 and 129 frames in Hunyuan at a resolution of 768×1280. To evaluate the acceleration effect achieved through the exploitation of attention sparsity by Compact Attention, we measured video quality using SSIM, PSNR, MSE and six quality metrics (Subject Consistency, Background Consistency, Aesthetic Quality) in VBench, and CLIPSIM and CLIPTemp (CLIP-T) [27] to measure the text-video alignment on Open-Sora benchmark. For computational performance, we report both the attention sparsity rate and attention latency. Compact Attention is implemented based on ThunderKittens, with reference to the STA framework.

**Baselines:** We evaluated Compact Attention against several state-of-the-art sparse attention approaches, including STA (spatio-temporal locality), Sparse VideoGen (static pattern), and Sparse Attention (dynamic pattern). For performance comparison, we measured similarity relative to full attention and quantified speedup using FlashAttention-2[7]. Additional implementation details can be found in Appendix C.

### 5.2 Acceleration Performance and Quality Preservation

**Similarity** Tab. 1 illustrates the sparsity efficiency of Compact Attention during end-to-end video inference within the Wan2.1 and Hunyuan model framework. A comparative analysis with various sparsity methods shows that Compact Attention achieves a superior acceleration ratio (2.51× speedup)

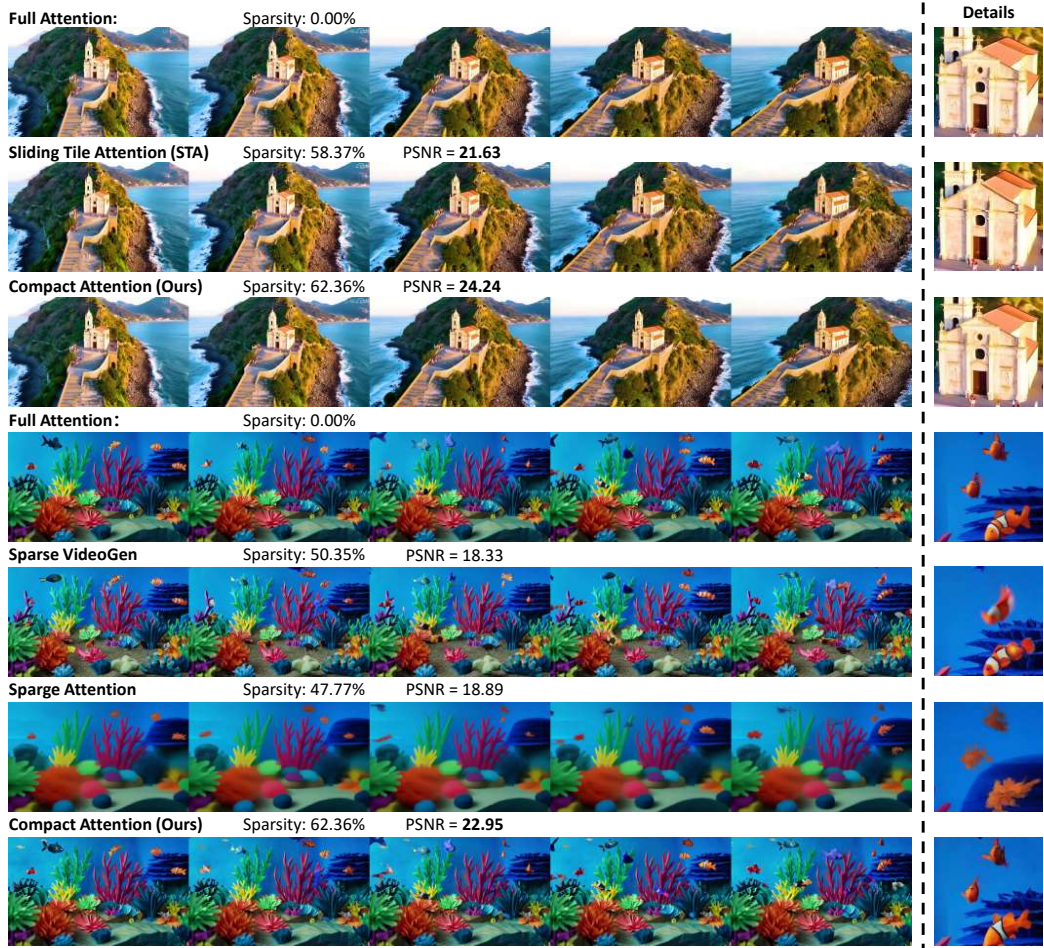


Figure 6: Performance of different sparse attention methods on end-to-end video generation.

in hunyuan at a higher sparsity level (62.36%) while maintaining high-quality generation, as reflected by a average PSNR of **30.0822**. This performance significantly surpasses baseline approaches: Sparse VideoGen experiences substantial quality degradation (PSNR 20.4297 at 50.35% sparsity) due to its uniform sparsity allocation across attention heads, whereas Sparge Attention, which employs dynamic block sparsity based on cosine similarity thresholds, exhibits limited stability despite its adaptive top- $k$  selection strategy.

**Quality** Table 2 evaluates sparse attention methods using selected VBench metrics. In some cases, text-video alignment is not meaningful to assess, as outputs from certain sparse attention variants deviate significantly from the original content. While videos from SpargeAttn exhibit low visual quality, both Sparse VideoGen and Compact Attention even outperform the full attention baseline on some metrics.

Fig. 6 presents the visual performance of various sparse attention methods on Hunyuan. Due to strict resolution constraints in STA, all methods are evaluated on 117-frame videos for consistency. While STA significantly improves generation speed, it suffers from notable quality degradation in Wan2.1. And in Hunyuan, our proposed Compact Attention achieves the miner impact on visual quality with higher sparsity. Results are also shown in Fig. 11, which demonstrates the superior performance of Compact Attention compared with Sliding Tile Attention (STA) in the Hunyuan video generation framework.

Table 3: Sparsity of different sparse pattern methods. Method of Sliding tile window uses a cubic window as an attention mask. In our method, we propose frame-group-wise masks and dual window to deal with time-variant heads and cross-shaped pattern separately, achieving 9.8% more sparsity when using params  $\tau = 0.9$  and  $\lambda = 0.011$  in searching.

Pattern	Cubic window + Frame-group-wise Patterns + Dual Windows
locality Patterns	0.726
cross Patterns	0.385
global Patterns	0.078
Time-Variant Patterns	0.441
Time-Invariant Patterns	0.306
<b>Overall</b>	<b>0.361</b>
	<b>0.370</b>
	<b>0.459</b>

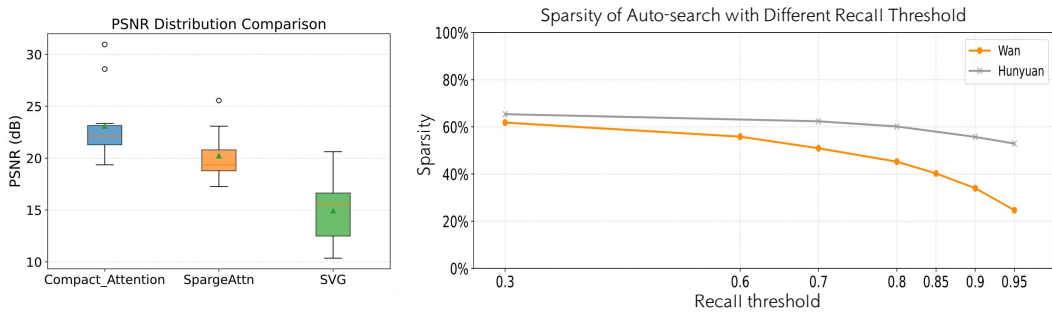


Figure 7: (a) Distribution of PSNR values across different parameter groups under diverse text prompts and random seeds. (b) Sparsity trends under different recall thresholds for auto-searched attention patterns on Wan2.1 and Hunyuan.

### 5.3 Ablation Studies

**Sparse Pattern Effectiveness** To validate the effectiveness of our proposed tile-based window with temporal difference in exploiting more sparsity for 3D full attention, We conduct experiments on the attention heads obtained during the inference phase of Wan2.1 and categorize them into different groups to analyze the detailed improvements within each pattern. The results show that the Dual Attention Windows increase the sparsity of cross patterns by approximately 10%, while the frame-group-wise pattern, which enables variation across the temporal dimension, contributes an additional improvement of around 3%.

## 6 Discussion: Robustness and Generalization

### 6.1 Stability Across Input Conditions

Fig. 7 presents the distribution of PSNR values obtained under varying input conditions, including diverse text prompts and random initialization seeds, across different parameter configurations and model variants. Notably, the configuration labeled Compact\_Attention—corresponding to sparsity parameters ( $\tau = 0.9$ ,  $\lambda = 0.011$ )—exhibits the highest median and mean PSNR values, along with a relatively narrow interquartile range. This indicates that it consistently delivers high-quality outputs with limited variance across stochastic or semantic input perturbations.

### 6.2 Sensitivity to Recall Threshold in Auto-search

As shown in Fig. 7, we analyze the sparsity patterns under varying recall thresholds (with fixed cost thresholds: 0.011 for Wan and 0.04 for Hunyuan). The results reveal that: Hunyuan, as a smaller model, consistently achieves higher attention sparsity than Wan. And with fixed cost threshold, the sparsity converges to an upper bound determined by the cost constraint when recall threshold

decreases. This suggests the need to carefully balance between acceleration (higher sparsity) and generation quality (lower recall threshold) in parameter selection.

### 6.3 Sensitivity to Sparsification in Early Denoising Steps

Our analysis of the denoising process reveals that sparse attention is most sensitive during the early stages, where high-noise inputs require structural initialization. Quantitative results show a 1.02dB PSNR drop when full attention is applied only in the final 15 steps, compared to the first 15. This highlights the importance of preserving full attention in the early timesteps to ensure quality, while allowing sparsification in later stages for acceleration without compromising visual fidelity. As is partly shown in Fig. 8, our empirical results suggest that maintaining full attention for the initial 15 denoising timesteps proves essential for preserving generation quality, whereas applying sparse attention in the remaining steps achieves notable acceleration with minimal quality loss.

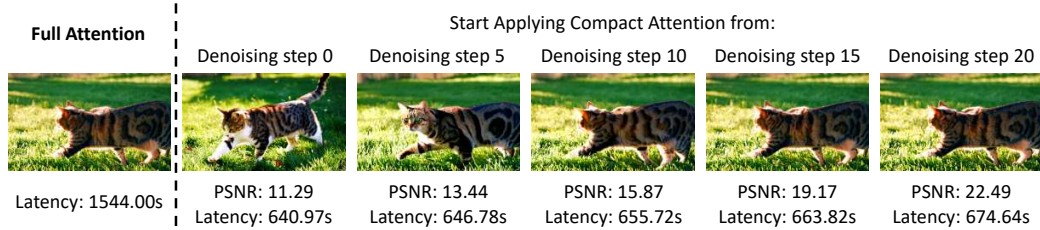


Figure 8: Effect of delaying sparse attention application: PSNR score and visual performance of sparse attention versus full attention.

## 7 Conclusion

The high computational cost of video generation models necessitates efficient spatiotemporal attention mechanisms that maintain generation quality. Through systematic analysis, we identify structured sparsity patterns in video diffusion transformers, including (1) local, cross-shaped, and global patterns in spatial dimensions, and (2) time-variant or time-invariant patterns in temporal dimensions. To leverage these patterns, we propose Compact Attention, which introduces three key innovations: (1) tile-based computation optimized for heterogeneous sparsity structures, (2) an automated mask search algorithm with cross-prompt merging for adaptive pattern selection. Extensive experiments on HD video generation show that our method achieves a 2.5 $\times$  speedup compared to full attention while preserving visual quality. This work presents a principled framework for co-designing sparse operators based on empirical attention characteristics, with potential applications in multimodal generation and real-time streaming systems.

## References

- [1] Shubham Agarwal et al. “Approximate caching for efficiently serving {Text-to-Image} diffusion models”. In: *21st USENIX Symposium on Networked Systems Design and Implementation (NSDI 24)*. 2024, pp. 1173–1189.
- [2] Fan Bao et al. “Analytic-dpm: an analytic estimate of the optimal reverse variance in diffusion probabilistic models”. In: *arXiv preprint arXiv:2201.06503* (2022).
- [3] Iz Beltagy, Matthew E Peters, and Arman Cohan. “Longformer: The long-document transformer”. In: *arXiv preprint arXiv:2004.05150* (2020).
- [4] Chaoxiang Cai et al. “Long-Tailed Distribution-Aware Router For Mixture-of-Experts in Large Vision-Language Model”. In: *arXiv preprint arXiv:2507.01351* (2025).
- [5] Zefan Cai et al. “Pyramidkv: Dynamic kv cache compression based on pyramidal information funneling”. In: *arXiv preprint arXiv:2406.02069* (2024).
- [6] Rewon Child et al. “Generating long sequences with sparse transformers”. In: *arXiv preprint arXiv:1904.10509* (2019).
- [7] Tri Dao et al. “FlashAttention: Fast and Memory-Efficient Exact Attention with IO-Awareness”. In: *Advances in Neural Information Processing Systems*. 2022, pp. 16344–16359.

- [8] Hangliang Ding et al. “Efficient-vDiT: Efficient Video Diffusion Transformers With Attention Tile”. In: *arXiv preprint arXiv:2502.06155* (2025).
- [9] Tianyu Fu et al. “Moa: Mixture of sparse attention for automatic large language model compression”. In: *arXiv preprint arXiv:2406.14909* (2024).
- [10] Zichuan Fu et al. “Sliding Window Attention Training for Efficient Large Language Models”. In: *arXiv preprint arXiv:2502.18845* (2025).
- [11] Yizhao Gao et al. “Seerattention: Learning intrinsic sparse attention in your llms”. In: *arXiv preprint arXiv:2410.13276* (2024).
- [12] Chi Han et al. “Lm-infinite: Zero-shot extreme length generalization for large language models”. In: *arXiv preprint arXiv:2308.16137* (2023).
- [13] Ali Hassani et al. “Generalized Neighborhood Attention: Multi-dimensional Sparse Attention at the Speed of Light”. In: *arXiv preprint arXiv:2504.16922* (2025).
- [14] Jonathan Heek, Emiel Hoogeboom, and Tim Salimans. “Multistep consistency models”. In: *arXiv preprint arXiv:2403.06807* (2024).
- [15] Huiqiang Jiang et al. “Minference 1.0: Accelerating pre-filling for long-context llms via dynamic sparse attention”. In: *Advances in Neural Information Processing Systems* 37 (2024), pp. 52481–52515.
- [16] Kumara Kahatapitiya et al. “Adaptive caching for faster video generation with diffusion transformers”. In: *arXiv preprint arXiv:2411.02397* (2024).
- [17] Dongjun Kim et al. “Consistency trajectory models: Learning probability flow ode trajectory of diffusion”. In: *arXiv preprint arXiv:2310.02279* (2023).
- [18] Nikita Kitaev, Łukasz Kaiser, and Anselm Levskaya. “Reformer: The efficient transformer”. In: *arXiv preprint arXiv:2001.04451* (2020).
- [19] Weijie Kong et al. “Hunyuanyvideo: A systematic framework for large video generative models”. In: *arXiv preprint arXiv:2412.03603* (2024).
- [20] Xunhao Lai et al. “FlexPrefill: A Context-Aware Sparse Attention Mechanism for Efficient Long-Sequence Inference”. In: *arXiv preprint arXiv:2502.20766* (2025).
- [21] Jiachen Li et al. “T2v-turbo: Breaking the quality bottleneck of video consistency model with mixed reward feedback”. In: *arXiv preprint arXiv:2405.18750* (2024).
- [22] Muyang Li et al. “Svdqunat: Absorbing outliers by low-rank components for 4-bit diffusion models”. In: *arXiv preprint arXiv:2411.05007* (2024).
- [23] Senmao Li et al. “Faster diffusion: Rethinking the role of unet encoder in diffusion models”. In: *CoRR* (2023).
- [24] Yucheng Li et al. “MAPSparse: Accelerating Pre-filling for Long-Context Visual Language Models via Modality-Aware Permutation Sparse Attention”. In: *ICLR 2025 Workshop on Foundation Models in the Wild*.
- [25] Enshu Liu et al. “Oms-dpm: Optimizing the model schedule for diffusion probabilistic models”. In: *International Conference on Machine Learning*. PMLR. 2023, pp. 21915–21936.
- [26] Luping Liu et al. “Pseudo numerical methods for diffusion models on manifolds”. In: *arXiv preprint arXiv:2202.09778* (2022).
- [27] Yaofang Liu et al. “Evalcrafter: Benchmarking and evaluating large video generation models”. In: *Proceedings of the IEEE/CVF Conference on Computer Vision and Pattern Recognition*. 2024, pp. 22139–22149.
- [28] Cheng Lu et al. “Dpm-solver: A fast ode solver for diffusion probabilistic model sampling in around 10 steps”. In: *Advances in Neural Information Processing Systems* 35 (2022), pp. 5775–5787.
- [29] Zhengyao Lv et al. “Fastercache: Training-free video diffusion model acceleration with high quality”. In: *arXiv preprint arXiv:2410.19355* (2024).
- [30] Xinyin Ma, Gongfan Fang, and Xinchao Wang. “Deepcache: Accelerating diffusion models for free”. In: *Proceedings of the IEEE/CVF conference on computer vision and pattern recognition*. 2024, pp. 15762–15772.
- [31] Xinyin Ma et al. “Learning-to-cache: Accelerating diffusion transformer via layer caching”. In: *Advances in Neural Information Processing Systems* 37 (2024), pp. 133282–133304.
- [32] Chenlin Meng et al. “On distillation of guided diffusion models”. In: *Proceedings of the IEEE/CVF Conference on Computer Vision and Pattern Recognition*. 2023, pp. 14297–14306.

[33] Jiezhong Qiu et al. “Blockwise self-attention for long document understanding”. In: *arXiv preprint arXiv:1911.02972* (2019).

[34] Luka Ribar et al. “Sparq attention: Bandwidth-efficient llm inference”. In: *arXiv preprint arXiv:2312.04985* (2023).

[35] Aurko Roy et al. “Efficient content-based sparse attention with routing transformers”. In: *Transactions of the Association for Computational Linguistics* 9 (2021), pp. 53–68.

[36] Tim Salimans and Jonathan Ho. “Progressive distillation for fast sampling of diffusion models”. In: *arXiv preprint arXiv:2202.00512* (2022).

[37] Axel Sauer et al. “Adversarial diffusion distillation”. In: *European Conference on Computer Vision*. Springer. 2024, pp. 87–103.

[38] Prajwal Singhania et al. “Loki: Low-rank keys for efficient sparse attention”. In: *arXiv preprint arXiv:2406.02542* (2024).

[39] Jiaming Song, Chenlin Meng, and Stefano Ermon. “Denoising diffusion implicit models”. In: *arXiv preprint arXiv:2010.02502* (2020).

[40] Yang Song et al. “Consistency models”. In: (2023).

[41] Hongyin Tang et al. “Ltri-LLM: Streaming Long Context Inference for LLMs with Training-Free Dynamic Triangular Attention Pattern”. In: *arXiv preprint arXiv:2412.04757* (2024).

[42] Yi Tay et al. “Sparse sinkhorn attention”. In: *International conference on machine learning*. PMLR. 2020, pp. 9438–9447.

[43] Team Wan et al. “Wan: Open and advanced large-scale video generative models”. In: *arXiv preprint arXiv:2503.20314* (2025).

[44] Hanrui Wang, Zhekai Zhang, and Song Han. “Spatten: Efficient sparse attention architecture with cascade token and head pruning”. In: *2021 IEEE International Symposium on High-Performance Computer Architecture (HPCA)*. IEEE. 2021, pp. 97–110.

[45] Felix Wimbauer et al. “Cache me if you can: Accelerating diffusion models through block caching”. In: *Proceedings of the IEEE/CVF Conference on Computer Vision and Pattern Recognition*. 2024, pp. 6211–6220.

[46] Haocheng Xi et al. “Sparse VideoGen: Accelerating Video Diffusion Transformers with Spatial-Temporal Sparsity”. In: *arXiv preprint arXiv:2502.01776* (2025).

[47] Yifei Xia et al. “Training-free and Adaptive Sparse Attention for Efficient Long Video Generation”. In: *arXiv preprint arXiv:2502.21079* (2025).

[48] Chaojun Xiao et al. “Inflm: Training-free long-context extrapolation for llms with an efficient context memory”. In: *arXiv preprint arXiv:2402.04617* (2024).

[49] Guangxuan Xiao et al. “Duoattention: Efficient long-context llm inference with retrieval and streaming heads”. In: *arXiv preprint arXiv:2410.10819* (2024).

[50] Guangxuan Xiao et al. “Efficient streaming language models with attention sinks”. In: *arXiv preprint arXiv:2309.17453* (2023).

[51] Qingsong Xie et al. “Mlcめ: Multistep consistency distillation of latent diffusion model”. In: *arXiv e-prints* (2024), arXiv–2406.

[52] Shang Yang et al. “Lserve: Efficient long-sequence llm serving with unified sparse attention”. In: *arXiv preprint arXiv:2502.14866* (2025).

[53] Shuo Yang et al. “Post-training sparse attention with double sparsity”. In: *arXiv preprint arXiv:2408.07092* (2024).

[54] Xinhao Yang et al. “PARO: Hardware-Software Co-design with Pattern-aware Reorder-based Attention Quantization in Video Generation Models”. In: *Des. Automat. Conf.* 2025.

[55] Tianwei Yin et al. “Improved distribution matching distillation for fast image synthesis”. In: *Advances in neural information processing systems* 37 (2024), pp. 47455–47487.

[56] Tianwei Yin et al. “One-step diffusion with distribution matching distillation”. In: *Proceedings of the IEEE/CVF conference on computer vision and pattern recognition*. 2024, pp. 6613–6623.

[57] Manzil Zaheer et al. “Big bird: Transformers for longer sequences”. In: *Advances in neural information processing systems* 33 (2020), pp. 17283–17297.

[58] Jintao Zhang et al. “Sageattention: Accurate 8-bit attention for plug-and-play inference acceleration”. In: *arXiv preprint arXiv:2410.02367* (2024).

[59] Jintao Zhang et al. “SageAttention2 Technical Report: Accurate 4 Bit Attention for Plug-and-play Inference Acceleration”. In: *arXiv preprint arXiv:2411.10958* (2024).

- [60] Jintao Zhang et al. “Spurgeattn: Accurate sparse attention accelerating any model inference”. In: *arXiv preprint arXiv:2502.18137* (2025).
- [61] Peiyuan Zhang et al. “Fast Video Generation with Sliding Tile Attention”. In: *arXiv preprint arXiv:2502.04507* (2025).
- [62] Qinsheng Zhang and Yongxin Chen. “Fast sampling of diffusion models with exponential integrator”. In: *arXiv preprint arXiv:2204.13902* (2022).
- [63] Zhenyu Zhang et al. “H2o: Heavy-hitter oracle for efficient generative inference of large language models”. In: *Advances in Neural Information Processing Systems* 36 (2023), pp. 34661–34710.
- [64] Tianchen Zhao et al. “Vidit-q: Efficient and accurate quantization of diffusion transformers for image and video generation”. In: *arXiv preprint arXiv:2406.02540* (2024).
- [65] Qianchao Zhu et al. “SampleAttention: Near-Lossless Acceleration of Long Context LLM Inference with Adaptive Structured Sparse Attention”. In: *arXiv preprint arXiv:2406.15486* (2024).

## A Limitations

The proposed auto-search strategy offers computational efficiency. However, through low recall and cost thresholds, this design choice may potentially compromise the visual fidelity of generated video content. Specifically, under more demanding scenarios, critical visual details could be omitted, leading to suboptimal generation quality. Future work will explore adaptive thresholding and context-aware search strategies to better balance efficiency and perceptual performance.

## B Broader Impacts

Our work reduces computational barriers for deploying long-video generation models through accelerated inference and lower memory costs, enabling broader access to high-quality video synthesis for individual creators and small teams. This democratization could catalyze innovation in education, digital art, and low-resource creative industries. Notably, our discovery of hierarchical attention patterns—such as localized spatial focus(local pattern, cross-shaped pattern), temporally-varying frame dependencies provides new insights into how video Transformers model spatiotemporal relationships. These patterns reveal specialized roles of attention heads (e.g., handling short-term motion or global context), improving model interpretability and offering a foundation for future research. Such findings could inspire targeted architectural designs (e.g., hybrid sparse attention modules) or curriculum learning strategies that align training with inherent spatiotemporal priors, potentially advancing both efficiency and controllability in video generation systems.

## C Baseline Implementation Details

**STA** STA is implemented based on FlashAttention-3 within the ThunderKittens framework and is compatible exclusively with the Hopper architecture. We adopt the publicly released mask configuration for Wan2.1 and Hunyuan from the official STA repository. Due to STA’s strict constraints on video resolution, all experiments are conducted on 69-frame or 117-frame videos at a resolution of 768×1280 using the STA kernel for fair comparison.

**SpARGE Attention** SpARGE Attention provides an interface for sparse attention operations via its open-source implementation. In our experiments, we integrate this interface into the diffusers library and evaluate the method using its default hyperparameters ( $\text{simthreshd}=0.1$ ,  $\text{cdfthreshd}=0.9$ ,  $\text{pvthreshd}=20$ ). The observed average sparsity is comparable to that of other baseline methods.

**Sparse VideoGen** We conduct experiments using the official implementation of Sparse VideoGen (SVG) from its open-source repository. The observed average sparsity is adjusted to be comparable to that of other baseline methods.

## D Sparsity Validation after rearranged based on adjacent 3D tiles

FlashAttention tiles the query, key, and value tensors along the token dimension into blocks  $Q_i$ ,  $K_i$ ,  $V_i$  with block sizes  $b_q$ ,  $b_k$  respectively, and computes each output block  $O_i$  incrementally using an online softmax[7]. This design achieves lower memory consumption and faster execution, while enabling attention acceleration through tile-level sparsity, thus avoiding the inefficiency of token-level sparsity. As a result, many sparse attention methods adopt small blocks as the basic computation unit. However, applying block-wise sparsity directly on attention over sequences obtained by flattening a 3D feature map (f, h, w) may be suboptimal, as it treats tokens within each block as equally important, regardless of spatial relationships. In Fig. 9 and Fig. 10, We show that reordering tokens based on 3D spatial locality prior to applying block-wise sparsity also improves attention sparsity while maintaining acceleration benefits in hunyuan. This spatially-aware grouping yields a **1%** reduction in the average number of active blocks on the Wan2.1 (14B) model, and **3.4%** on the Hunyuan model.

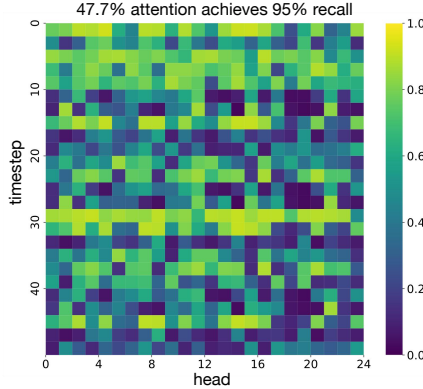


Figure 9: Flattening sequence on tiles

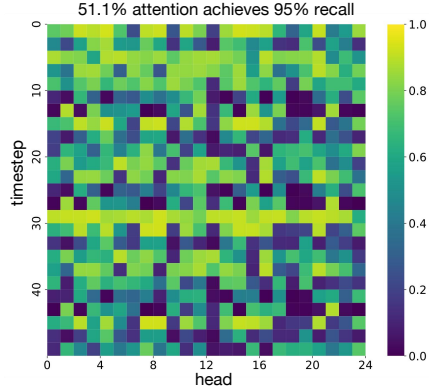


Figure 10: Directly flattening sequence

## E Additional Experiment Results

### E.1 Comparative Analysis with Baseline Methods

Fig. 11 demonstrates the superior performance of Compact Attention compared with Sliding Tile Attention (STA) in the Hunyuan video generation framework. Our method achieves enhanced Peak Signal-to-Noise Ratio (PSNR) while operating at higher sparsity rates. Specifically, to accommodate STA’s tile grouping requirements for attention sequence processing, we conducted comparative evaluations using 117-frame video sequences. The visual comparisons reveal that Compact Attention maintains better video quality preservation despite increased sparsity levels, confirming that our approach more effectively identifies and retains critical attention computation components - a core design principle of our architecture. Furthermore, we extended the comparison to include Sparge Attention and Sparse VideoGen using the standard 129-frame sequences recommended for optimal video generation performance as shown in Fig. 12. While these baseline methods employ dynamic and static sparsification strategies respectively, neither sufficiently addresses the precise identification of computationally critical attention regions. As evidenced by the quantitative metrics, Compact Attention exhibits significant advantages in video quality retention metrics under comparable sparsity conditions. This performance gap highlights our method’s improved capability in preserving essential spatial-temporal attention patterns through systematic sparse computation. More generation cases are shown in Fig. 13.

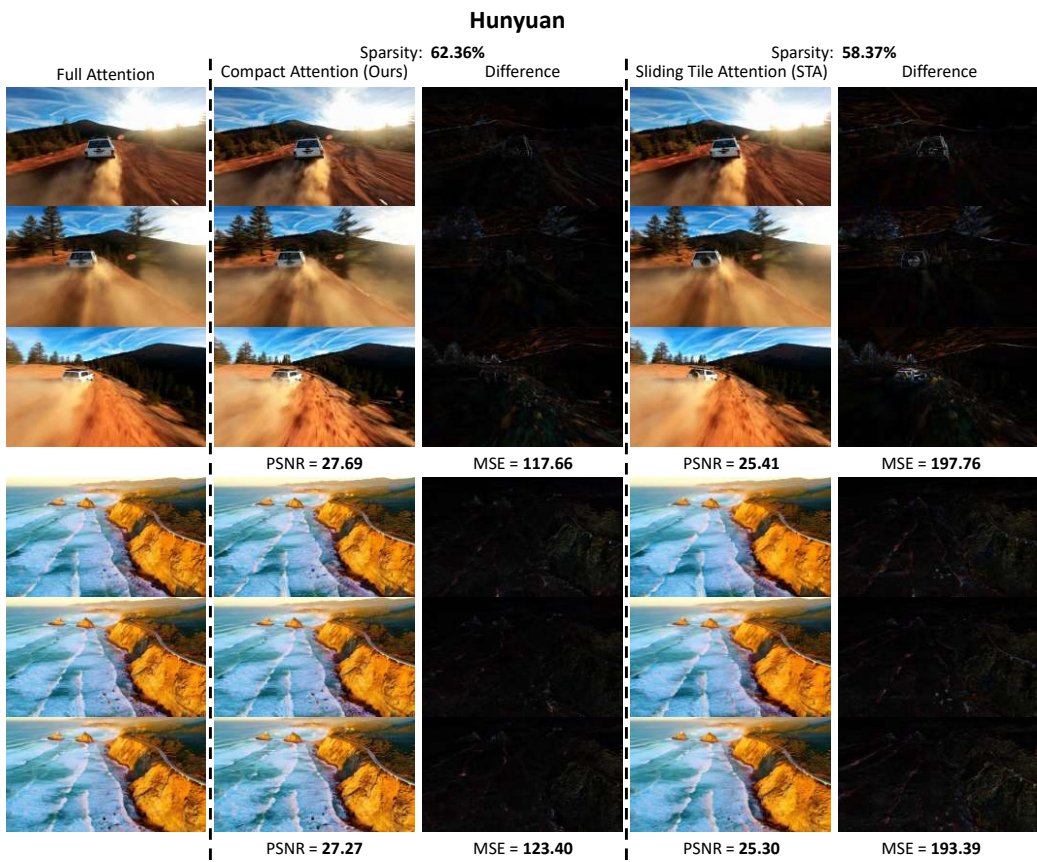


Figure 11: Performance of Compact Attention and Sliding Tile Attention on end-to-end video generation.

## Hunyuan

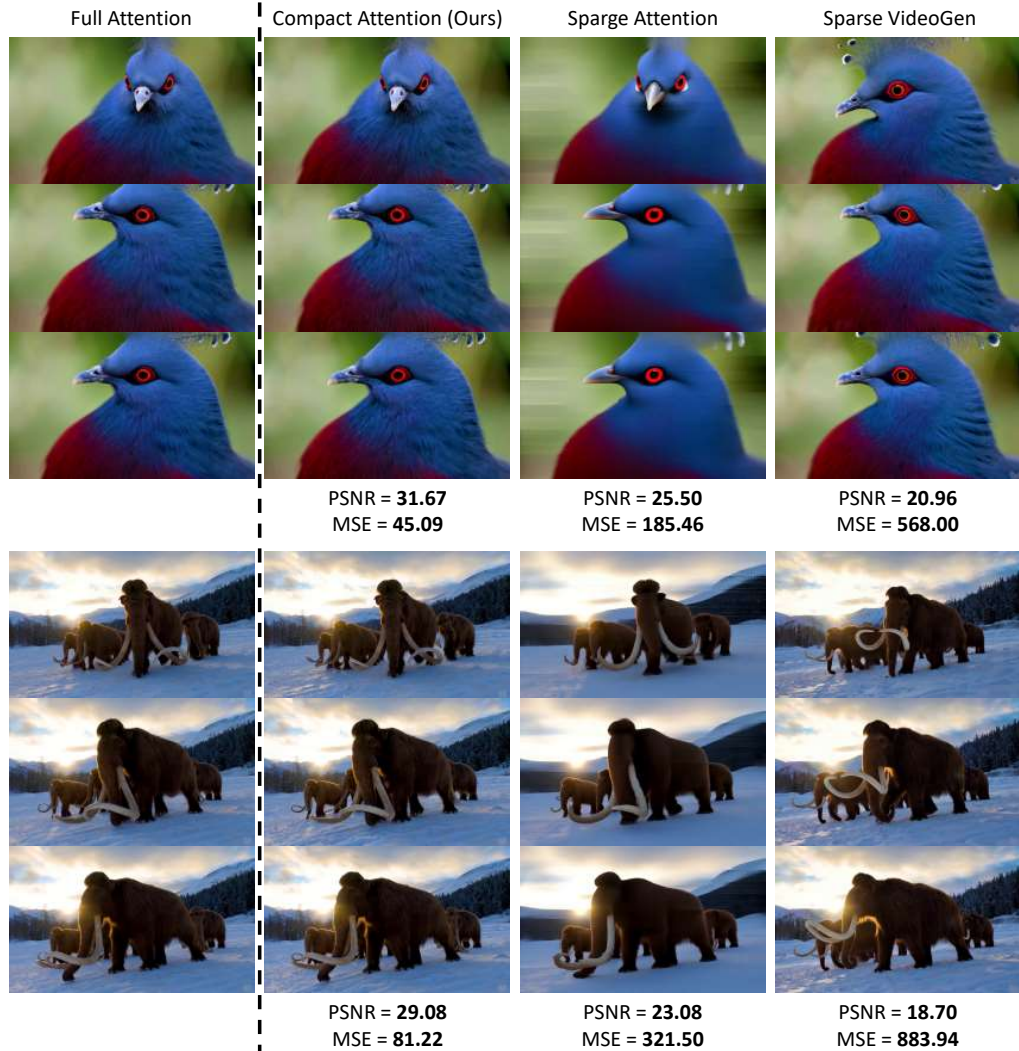


Figure 12: Performance of Compact Attention and baselines on end-to-end video generation.

Hunyuan

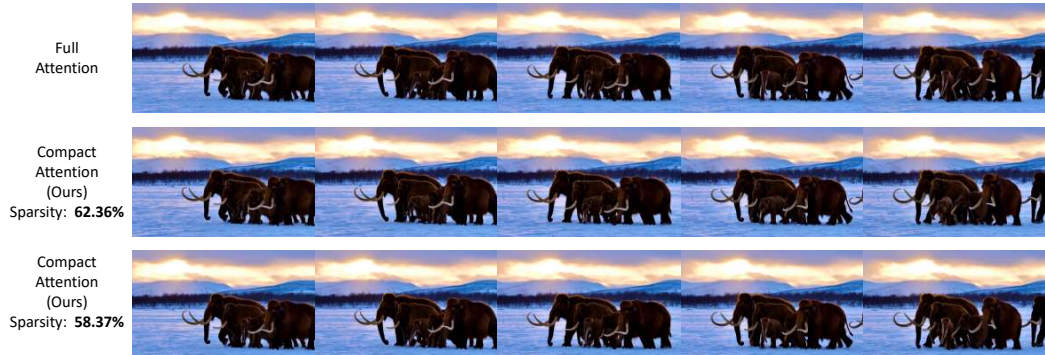


Figure 13: Performance of Compact Attention on end-to-end video generation.